



**HAL**  
open science

# Electrospinning fabrication of polystyrene-silica hybrid fibrous membrane for high-efficiency air filtration

Hongzhe Tang, Dong Han, Jian Zhang

► **To cite this version:**

Hongzhe Tang, Dong Han, Jian Zhang. Electrospinning fabrication of polystyrene-silica hybrid fibrous membrane for high-efficiency air filtration. *Nano Express*, 2021, 2 (2), pp.020017. 10.1088/2632-959X/abfe3d . hal-03777593

**HAL Id: hal-03777593**

**<https://hal.science/hal-03777593>**

Submitted on 14 Sep 2022

**HAL** is a multi-disciplinary open access archive for the deposit and dissemination of scientific research documents, whether they are published or not. The documents may come from teaching and research institutions in France or abroad, or from public or private research centers.

L'archive ouverte pluridisciplinaire **HAL**, est destinée au dépôt et à la diffusion de documents scientifiques de niveau recherche, publiés ou non, émanant des établissements d'enseignement et de recherche français ou étrangers, des laboratoires publics ou privés.



Distributed under a Creative Commons Attribution 4.0 International License

PAPER • OPEN ACCESS


# Electrospinning fabrication of polystyrene-silica hybrid fibrous membrane for high-efficiency air filtration

To cite this article: Hongzhe Tang *et al* 2021 *Nano Ex.* 2 020017

View the [article online](#) for updates and enhancements.

## You may also like

- [Air filtration media from electrospun waste high-impact polystyrene fiber membrane](#)  
Akmal Zulfi, Muhammad Miftahul Munir, Dian Ahmad Hapidin *et al.*
- [Biogenic synthesis of nano-sulfur using \*Punica granatum\* fruit peel extract with enhanced antimicrobial activities for accelerating wound healing](#)  
K Samrat, M N Chandrababha, R Hari Krishna *et al.*
- [Moisture and temperature influences on nonlinear vegetation trends in Serengeti National Park](#)  
Ningyuan Huang, Pinki Mondal, Benjamin I Cook *et al.*



**ECS** The Electrochemical Society  
Advancing solid state & electrochemical science & technology

## 242nd ECS Meeting

Oct 9 – 13, 2022 • Atlanta, GA, US

Presenting more than 2,400 technical abstracts in 50 symposia

**Register now!**

**ECS Plenary Lecture featuring M. Stanley Whittingham,**  
Binghamton University  
Nobel Laureate –  
2019 Nobel Prize in Chemistry

The banner features a portrait of M. Stanley Whittingham, a Nobel Prize medal, and a background image of a person interacting with a futuristic interface.



## PAPER

## OPEN ACCESS

## Electrospinning fabrication of polystyrene-silica hybrid fibrous membrane for high-efficiency air filtration

RECEIVED  
22 December 2020REVISED  
25 April 2021ACCEPTED FOR PUBLICATION  
5 May 2021PUBLISHED  
14 May 2021

Original content from this work may be used under the terms of the [Creative Commons Attribution 4.0 licence](#).

Any further distribution of this work must maintain attribution to the author(s) and the title of the work, journal citation and DOI.

Hongzhe Tang<sup>1,2</sup>, Dong Han<sup>2,3,\*</sup>  and Jian Zhang<sup>4,\*</sup> <sup>1</sup> Hangzhou Innovation Institute Yuhang, Beihang University, 310000, Hangzhou, People's Republic of China<sup>2</sup> Creuzet Laboratory, Ecole Centrale de Pékin, Beihang University, 100191, Beijing, People's Republic of China<sup>3</sup> Institut des Nanotechnologies de Lyon, CNRS UMR 5270, Ecole Centrale de Lyon, University of Lyon, 69134 Ecully Cedex, France<sup>4</sup> Institut Charles Gerhardt de Montpellier, UMR CNRS 5253 Université de Montpellier-CNRS-ENSCM, Place Eugène Bataillon, 34095 Montpellier Cedex 05, France

\* Authors to whom any correspondence should be addressed.

E-mail: [handong@buaa.edu.cn](mailto:handong@buaa.edu.cn) and [jian.zhang@doctorant.ec-lyon.fr](mailto:jian.zhang@doctorant.ec-lyon.fr)**Keywords:** fibrous membrane, electrospinning, air filtration, polystyrene, silicaSupplementary material for this article is available [online](#)**Abstract**

The development of new materials for air filtration and particulate matter (PM) pollution is critical to solving global environmental issues that threaten human health and accelerate the greenhouse effect. In this study, a novel electrospun polystyrene-SiO<sub>2</sub> nanoparticle (PS-SNP) fibrous membrane was explored by a single-step strategy to obtain the composite multi-layered filter masks. In addition, the air filtration performance of this fibrous membrane for PM was evaluated. The effects of SiO<sub>2</sub> on the composition, morphology, mechanical property, and surface wetting of PS-SNP membranes were studied. Allowing SiO<sub>2</sub> to be incorporated into the PS polymer was endowed with promising superhydrophobicity and demonstrated excellent mechanical properties. As-prepared PS-SNP membranes possess significantly better filtration efficiency than pure PS membrane. Furthermore, a three-layered air filter media (viscose/PS-SNP/polyethylene terephthalate) used in this study has considerable performances compared to the commercial masks. Since this air filtration membrane has excellent features such as high air filtration and permeability, we anticipate it to have huge potential application in air filtration systems, including cleanroom, respirator, and protective clothing.

**1. Introduction**

In the past ten years, the problem of air pollution is becoming more and more serious. Many pollutants such as PM<sub>2.5</sub> and PM<sub>10</sub> are produced by coal use and combustion of fossil fuel [1]. Most areas of industrial cities and their surroundings often appear of fog and haze weather, and in the short term, it is difficult to be improved obviously. Particles represented by PM<sub>2.5</sub> can enter alveoli and blood, which causes irreversible effects on human health [2–5]. As people's awareness of self-protection is gradually increased, all kinds of anti-haze respirators are emerging. Besides, a recent outbreak of novel coronavirus pneumonia has spread rapidly around the globe [6–8]. The World Health Organization (WHO) recommends using masks as a set of public health interventions to prevent and control the spread of certain viral respiratory diseases [9]. Therefore, the design and research of high-efficiency filtration membrane used in the mask or other filtration devices is a central focus.

It is well known that electrospinning is an effective and environmentally friendly method that is widely used in producing continuous fiber membrane fields [10–13]. The prepared membrane exhibits controllable fiber diameter and controllable porous structure, making it an ideal choice for air filtration materials. According to these characteristics, many materials used for electrospun fiber membranes, such as polyurethane (PU), poly(acrylic acid) (PAA), polyethyleneimine (PEI), polyvinyl acetate (PVA), and polyacrylonitrile (PAN), have been reported [13–17]. Polystyrene (PS), a kind of colorless thermoplastic plastic, has a wide range of applications in the field of chemistry, life sciences, and medical treatment when it is prepared into fibrous membranes [18–21].

Electrospun fibers usually have a relatively smooth surface, which greatly influences the filtration properties of membranes. Allowing nano-inorganic materials to be incorporated into fibers membrane has been a widely-used method to construct hybrid structures and increase materials roughness. There are three methods to integrate inorganic materials into fibrous membrane: (i) 'pre-add' mixing nanomaterials to a spinning solution before electrospinning [22]; (ii) 'after-grow' *in situ* synthesis nanomaterials after membrane electrospinning [23]; (iii) 'multi-jet' electrospinning of nanomaterial dispersions and simultaneous electrospinning of polymer solutions [24]. Hybrid fibrous membranes with inorganic materials using the electrospinning method exhibit good filtration efficiency. For example, Q Ke *et al* prepared hierarchically structured TiO<sub>2</sub>/PAN fibrous membranes, which showed excellent filtration efficiency and toluene degradation performance [25]. G Singh *et al* reported a polyvinylidene fluoride (PVDF)-Ag-Al<sub>2</sub>O<sub>3</sub> nanofibrous membrane, which exhibited not only excellent filtration efficiency but antibacterial and detoxifying properties [26]. Moreover, S Wong *et al* studied that a critical loading of nano-scale graphite platelets (NGP) within PVDF membranes could improve both filtration efficiency and pressure drop [27]. Besides, due to the excellent electret performance created by dipole orientation and charge storage, SiO<sub>2</sub> is considered a promising material for designing new fibrous materials for air filtration [28–30]. It could enhance the mechanical properties and hydrophobicity of polymer fibrous membranes. It was reported that the SiO<sub>2</sub> nanoparticle was incorporated into PAN or PEI fiber membranes by pre-adding nanoparticles into a spinning solution to enhance the filtration performance [22, 31].

In this work, SiO<sub>2</sub> nanoparticles (SNP) were incorporated by the electrospinning technology to controllably manufacture hierarchical polystyrene (PS) fiber membrane with strong filtration performance for the first time. In addition, the combination of SNP has a great influence on the morphology, surface wettability, and mechanical property of the resulting PS-SNP membranes. More significantly, the PS-SNP fibrous membrane was assembled with viscose and polyethylene terephthalate (PET) into a three-layered air filtration media, which exhibits comparable performances of air filterability and permeability compared with other mask products sold on the market.

## 2. Experiments

### 2.1. Materials

The polystyrene (PS,  $M_w = 192000$ ) was obtained from Sigma-Aldrich. The N, N-Dimethylformamide (DMF) was of analytical grade and supplied by Xilong Chemical Co., Ltd SiO<sub>2</sub> nanoparticles (with a diameter of 100 nm) were purchased from Beijing Chemical Reagents Co., Ltd. All reagents are used as received, no further purification is required.

### 2.2. Polymer solutions preparation

A PS solution (20 wt.%) was prepared by dissolving in DMF 24 h under stirring. SiO<sub>2</sub> nanoparticles (SNP) were then dispersed to this solution to prepare PS/SNP fibrous membranes. Additionally, PS solutions containing 0, 2, 5, 8, 10, and 12 wt.% SNP were prepared, respectively, using a DMF mixture.

### 2.3. Fabrication of PS/SNP fibrous membrane

The PS solution was loaded into a jet and injected through a metal needle at a feed rate of 3.0 ml h<sup>-1</sup>. Since a high voltage of 20 kV is applied to the needle tip, a continuous jet is generated. The PS fiber membrane was deposited on aluminium foil 20 cm from the tip of the syringe. Then, the obtained electrospun membrane was dried in a vacuum for 2 h to remove residual solvent. The PS/SNP hybrid fibrous membranes containing various contents of SNPs were denoted as PS-SNP<sub>x</sub> (where x is the mass ratio of SiO<sub>2</sub> nanoparticles in hybrid membranes).

### 2.4. Characterization

The PS and PS-SNP<sub>x</sub> membranes' morphologies were characterized using a scanning electron microscope (SEM, JSM7500, JEOL, Tokyo, Japan). The water contact angle measurements were performed using a water contact angle goniometer (JC2000C, Powereach Co., Shanghai, China). The mechanical properties were tested on a tensile tester (XQ-1C, Shanghai New Fiber Instrument Co., Ltd, China) at a crosshead speed of 5 mm per minute at room temperature. X-ray photoelectron spectroscopy (XPS) spectra were conducted using a VSW spectrometer equipped with a monochromatized X-ray source ( $Al K\alpha h\nu = 1486.6$  eV). The take-off angle was 90°, and the energetic resolution was 0.2 eV. Data analysis was performed with the CasaXPS software.

### 2.5. Air permeability and filtration performance

PS-SNP<sub>x</sub> electrospun fibrous membrane was assembled with viscose and polyethylene terephthalate (PET) into a three-layered structure (figure 1(a)). Viscose and PET non-woven fabric are the most commonly used materials for masks due to the physiological moisture requirement to human skin and having relatively good air

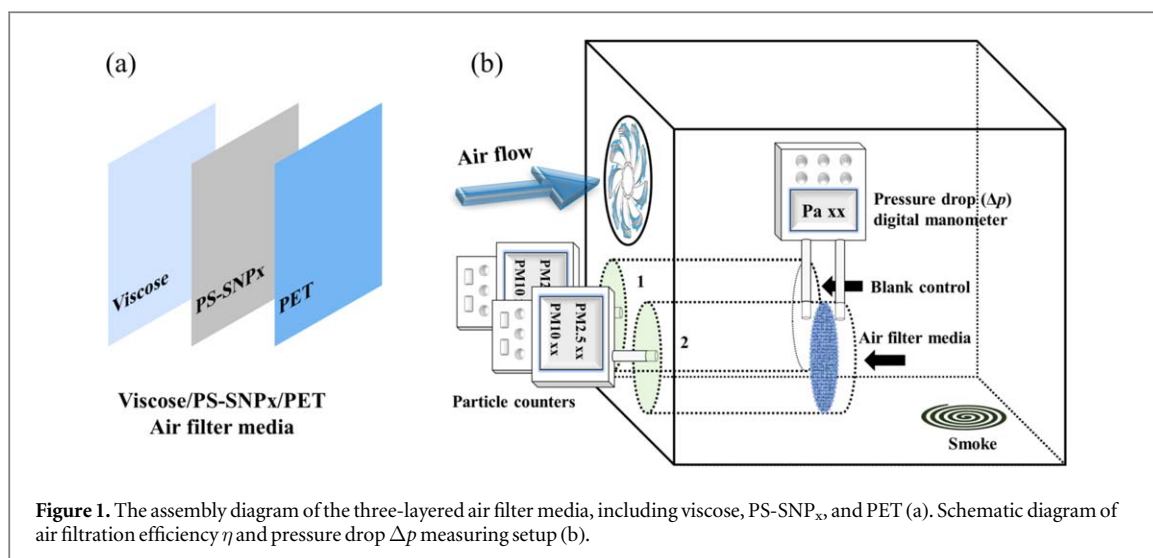


**Figure 1.** The assembly diagram of the three-layered air filter media, including viscose, PS-SNP<sub>x</sub>, and PET (a). Schematic diagram of air filtration efficiency  $\eta$  and pressure drop  $\Delta p$  measuring setup (b).

permeability. In this study, viscose was used as the inner layer, PET was used as the outer layer, our PS-SNP fibrous membranes were used as the middle layer. Therefore, the front and back sides of the PS-SNP fibrous membranes were covered with PET and viscose forming an air filter media. The edges of the three-layers film were fixed by nylon sewing thread to prevent interlayer peeling. An assembled sandwich-type air filter media (viscose/PS-SNP<sub>x</sub>/PET) was made to compare with the other sold masks on the market.

The air filtration and the pressure drop were performed in a homemade system (figure 1(b)). It shows a test setup composed of two chambers at the bottom of a container (25 cm  $\times$  35 cm  $\times$  50 cm). Chamber 1 is a cylindrical shaped structure (internal diameter 12.6 cm) with a hole (3 cm in diameter) at the left side for the particle counter. The right side is completely open to the container. Chamber 2 is identical to chamber 1. However, on the right side, the air filter media (viscose/PS-SNP<sub>x</sub>/PET) was well installed in the cylindrical shaped structure by tapes during the study to separate chamber 2 from the container. Hence, chamber 1 is a blank control structure compared with chamber 2. In addition, a smoke generator is located inside the container on the right side. Meanwhile, a blower is used to induce the airflow into the two processing chambers. In this work, the smoke (considered as the source of PM) was produced by burning a cigarette. Its smoke was firstly isolated in the container and then inhaled in all subsequent chambers during the filtration process. PM concentration was measured by particle counters (in  $\mu\text{g m}^{-3}$ , test X in HT9600) from chamber 1 (blank control) and chamber 2 (after air filter media), respectively. The environmental conditions were maintained at constants: 25 °C with a relative humidity of 60%. The air filtration efficiency ( $\eta$ ) was calculated using the equation (1) [12]

$$\eta = 1 - \frac{C_{\text{filter}}}{C_{\text{blank}}} \quad (1)$$

where  $C_{\text{blank}}$  is the concentration of PM2.5 taken from the blank control chamber 1 and  $C_{\text{filter}}$  is that taken from chamber 2 after the air filter media. The pressure drop ( $\Delta p$ ) was obtained by a digital manometer measuring the pressure difference across the sample (blue, marked in figure 1(b)) during filtration tests. To determine the overall performance of this air filter, the quality factor (QF) was calculated by the experimental data of filtration efficiency and pressure drop using the equation (2) [12]

$$\text{QF} = -\frac{\ln(1 - \eta)}{\Delta p} \quad (2)$$

### 3. Results and discussion

SEM images of the PS-SNP<sub>x</sub> with different amounts of SiO<sub>2</sub> nanoparticles are shown in figure 2. As observed, the prepared membranes exhibit an interconnected porous structure, and the fibers are randomly oriented. Figure 2(a) shows the very smooth surface morphology of pure PS fibers. However, after introducing SiO<sub>2</sub> nanoparticles (figures 2(b)–(f)), granular particles are dispersed on the surface of PS-SNP<sub>x</sub> fibers, which indicates that the SiO<sub>2</sub> nanoparticles have been successfully doped into the membrane. The PS-SNP<sub>x</sub> membranes contain hybrid fibers with an average diameter of approximately 2.5  $\mu\text{m}$  (figure S1, see supporting information (available online at [stacks.iop.org/NANOX/2/020017/mmedia](https://stacks.iop.org/NANOX/2/020017/mmedia))). It is obvious that the fiber diameters of different membranes are not much different, which indicates that the introduction of nanoparticles does not significantly change the diameter of the electrospun membranes. On the contrary, with the increase of

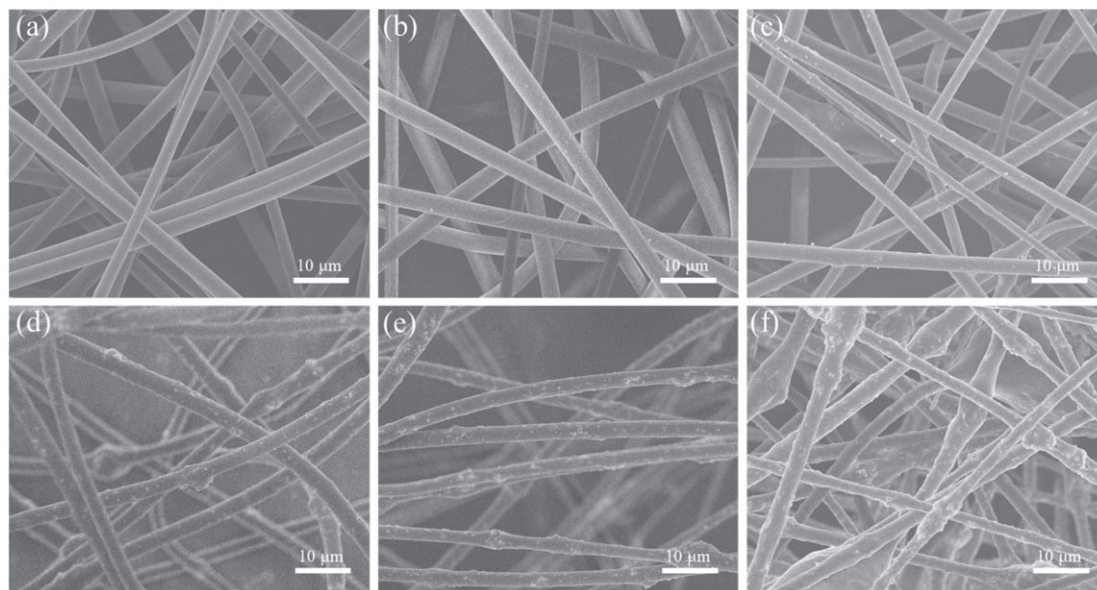


**Figure 2.** SEM images of PS-SNP<sub>x</sub> under different SiO<sub>2</sub> nanoparticles concentrations. (a) 0 wt.%; (b) 2 wt.%; (c) 5 wt.%; (d) 8 wt.%; (e) 10 wt.%; and (f) 12 wt.%.

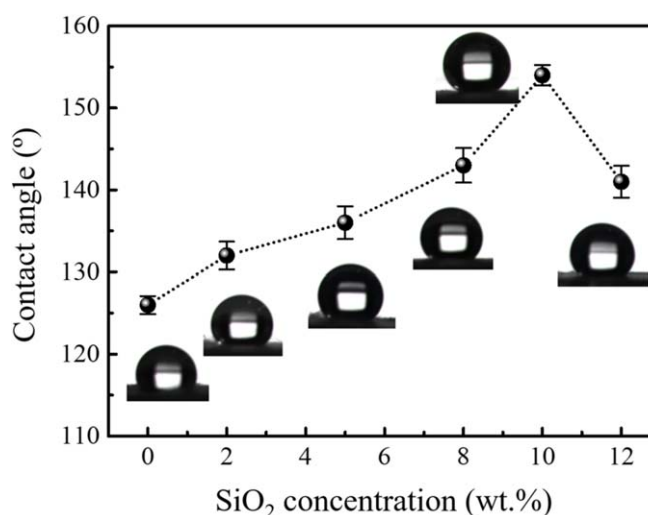


**Figure 3.** Variation of contact angle value of PS-SNP<sub>x</sub> membranes based on different weight ratios of SiO<sub>2</sub> nanoparticles.

SiO<sub>2</sub> content, the morphology of the fiber has been changed considerably. The more nano-scale protrusions were formed on the surface, the rougher the morphology of membranes became. It can be concluded that this work provides a simple method to construct structured membranes in which SiO<sub>2</sub> nanoparticles are distributed on fibers controlled by different amounts.

Figure 3 displays the water contact angle (CA) value of the PS-SNP membranes as a function of SiO<sub>2</sub> nanoparticle concentration. The wettability of the composite fiber membrane decreases with the increasing amount of SiO<sub>2</sub> nanoparticle from 0 to 10 wt.%. The CA increases from 126° to 155°, indicating a superhydrophobic surface. However, the CA of the fiber membrane drops to 140° when the amount of SiO<sub>2</sub> nanoparticle up to 12 wt.%, which is mainly based on the alternation of surface morphology. Initially, the pure PS fibers have very smooth surfaces (figure 1(a)). When SiO<sub>2</sub> is involved (2 wt.%), the nanoparticle attachment appears on the surface of the fibers, which begins to raise the roughness of PS-SNP membranes, so that the CA is improved. Continue to increase the SiO<sub>2</sub> concentration up to 10 wt.%, SiO<sub>2</sub> adhesion rate expands significantly. Simultaneously, a large number of grooves and edges appear, which amplifies the roughness of the film surface. Further increasing the SiO<sub>2</sub> concentration (12 wt.%), the CA value is decreased to 140°, probably resulting from that SiO<sub>2</sub> agglomeration phenomenon destroy the dual-scale structure and trap less air in surface cavities [32].

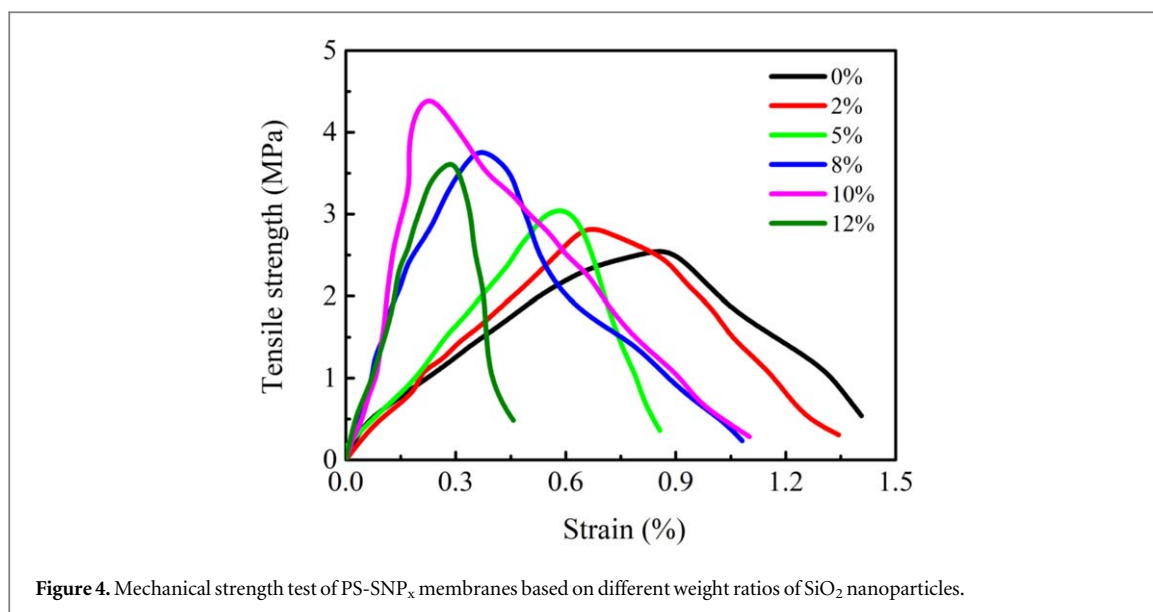


**Figure 4.** Mechanical strength test of PS-SNP<sub>x</sub> membranes based on different weight ratios of SiO<sub>2</sub> nanoparticles.

Besides, the introduction of hydrophilic SiO<sub>2</sub> nanoparticles affects the hydrophobicity of the PS-SNP membrane surface.

The tensile properties of pure PS and PS-SNP<sub>x</sub> membranes are shown in figure 4, where the maximum tensile strength variation and the stress-strain diagram are plotted. The mechanical properties values of the pure PS and PS-SNP<sub>x</sub> are given in table S1 (see supporting information). After adding SiO<sub>2</sub> nanoparticles, the tensile strength of the membrane is improved. The difference in each membrane strength-strain curve is mainly caused by SiO<sub>2</sub> content. Electrospun pure PS membranes are generally soft and flexible, with a tensile strength of less than 2.55 MPa. It can be seen that the increase of tensile strength is related to the presence of SiO<sub>2</sub>. Compared to pure PS membranes, the tensile strength of PS-SNP<sub>10</sub> composites is enhanced by 72% from 2.55 to 4.39 MPa. This improvement in mechanical properties is evidence of the transfer of efficient load to SiO<sub>2</sub> in PS-SNP<sub>x</sub> membranes. The enhancement of the mechanical property of PS-SNP<sub>x</sub> membranes has probably resulted from the strong interaction between PS and SiO<sub>2</sub>. Firstly, SiO<sub>2</sub> acts as a cross-linking point to associate with polymer chains, thereby increasing the rigidity. Secondly, the inorganic nanoparticles on the composite electrospun fiber rises the friction between adjacent fibers [33, 34]. Besides, the tensile strength of the membrane is slightly decreased at 12 wt.% SiO<sub>2</sub> content. This decrease could be attributed to the uneven distribution of SiO<sub>2</sub> in the polymer matrix, which leads to an aggregation of clay. These aggregates cause the stress to be concentrated at various points in the polymer, thereby reducing the mechanical properties. However, it is still higher than that of the pure PS membrane. The positive effect of SiO<sub>2</sub> depends largely on the dispersion of SiO<sub>2</sub> nanoparticles in the matrix and its interface interactions [35].

Apart from tensile mechanical properties, the bending ability is also a notable point in membrane or film materials [36, 37]. Because this is very important for the application of flexible devices and commodities. In this study, both PS and PS-SNP<sub>x</sub> membranes exhibit good flexibility during materials characterization and filtration tests. Figure S2 (see supporting information) shows an optical image of the fold PS-SNP<sub>10</sub> membrane. Although induced by SiO<sub>2</sub>, the PS-SNP membrane was flexible and no obvious cracks appeared. Additionally, as another determination of the flexibility, the bending rigidity test will also be considered in the follow-up work to provide more comprehensive proof.

X-ray photoelectron spectroscopy (XPS) is used to investigate surface compositions of the PS-SNP<sub>10</sub> membranes when the content of SiO<sub>2</sub> is 10 wt.%. For the pure PS membrane, the Si 2*p* and O 1*s* peaks were not detected as expected. However, they appear obviously on PS-SNP<sub>10</sub> membranes surface, as shown in figure 5. From the high-resolution Si 2*p* spectrum (figure 5(a)), the signal (103.5 eV) is due to the Si-O bond. The O 1*s* high-resolution spectrum shows two visible signals, the peak at a binding energy of 531.5 eV was related to the Si-O bond; another at a binding energy of about 533.3 eV was probably associated with the surface oxygen contamination (figure 5(b)) [38]. The XPS results indicate the incorporation of SiO<sub>2</sub> nanoparticles into the PS.

The filtration performance of the viscose/PS-SNP<sub>x</sub>/PET air filter media with various concentrations of SiO<sub>2</sub> nanoparticle is demonstrated in figure 6(a). It is worth noting that the PS-SNP<sub>x</sub> (*x* = 0, 5, 10, and 12 wt.%) membranes were assembled with viscose and polyethylene terephthalate (PET). In addition, the viscose/viscose/viscose and PET/PET/PET three-layered filter media were also prepared and compared as control. As shown in figure 6(a), the abscissa is the pressure drop ( $\Delta p$ ), and the ordinate is the filtration efficiency ( $\eta$ ). The filtration efficiency of viscose/PS-SNP<sub>x</sub>/PET membranes versus the increasing SiO<sub>2</sub> content of 0, 5, 10, and 12

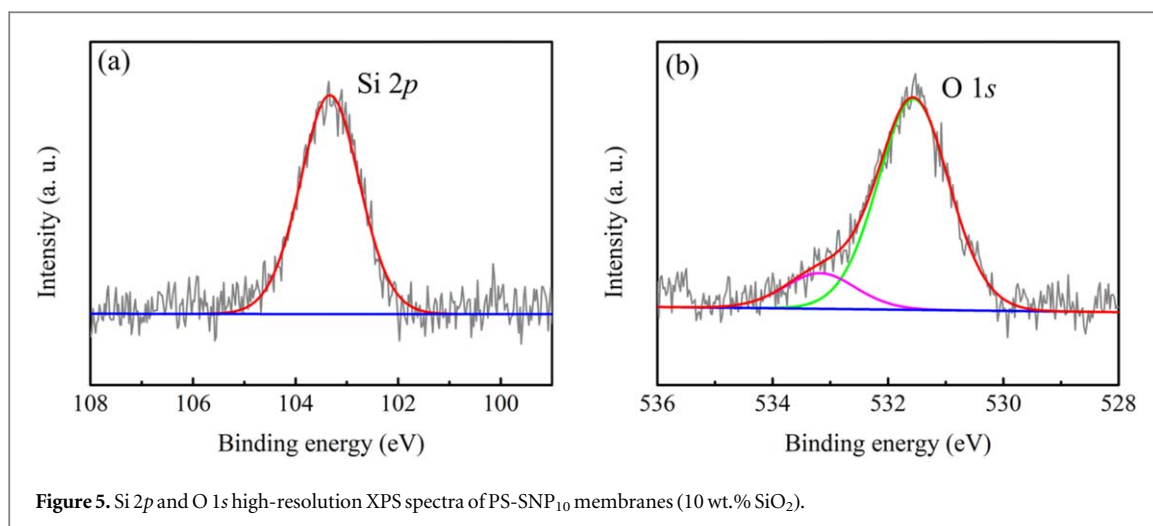


Figure 5. Si 2p and O 1s high-resolution XPS spectra of PS-SNP<sub>10</sub> membranes (10 wt.% SiO<sub>2</sub>).

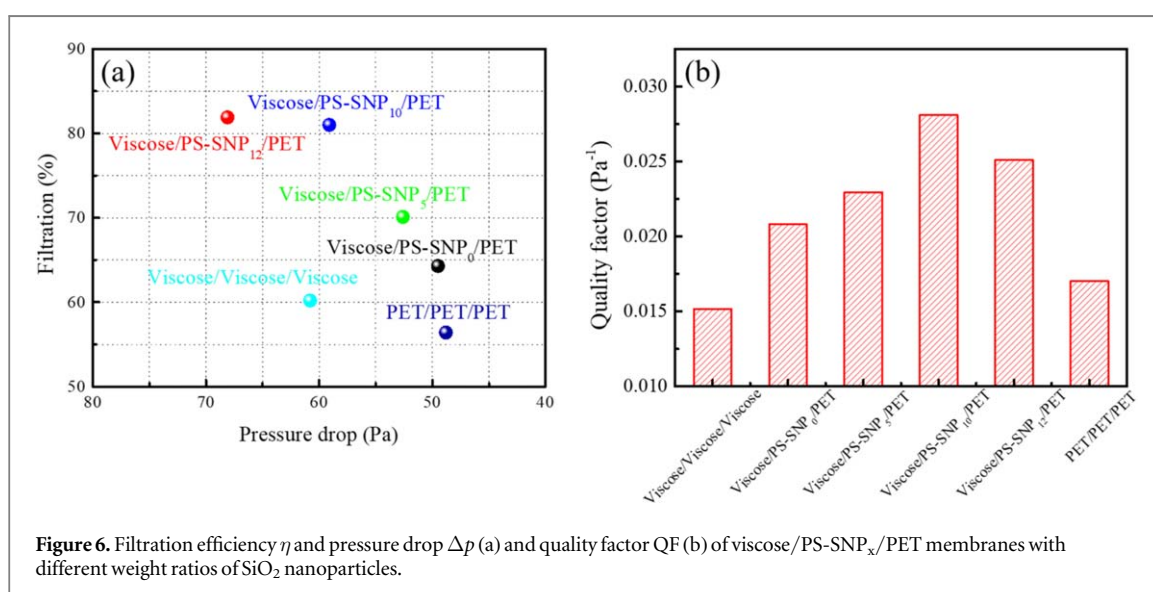


Figure 6. Filtration efficiency  $\eta$  and pressure drop  $\Delta p$  (a) and quality factor QF (b) of viscose/PS-SNP<sub>x</sub>/PET membranes with different weight ratios of SiO<sub>2</sub> nanoparticles.

wt.% are 64.3%, 70.1%, 81%, and 81.9% respectively, while the corresponding pressure drop are 49.5, 52.6, 59.1, and 68.1 Pa respectively. In this case, as more SiO<sub>2</sub> nanoparticles are incorporated into the PS-SNP, the values of both  $\Delta p$  and  $\eta$  gradually increase. Furthermore, although the viscose/PS-SNP<sub>12</sub>/PET shows the best efficiency ( $\eta = 81.9\%$ ), the  $\Delta p$  value is the highest among all samples, revealing the worst air permeability. The  $\eta$  of viscose/PS-SNP<sub>10</sub>/PET is about 81%, slightly lower than that of viscose/PS-SNP<sub>12</sub>/PET. However, its  $\Delta p$  value is about 59.1 Pa, which is much lower than that of viscose/PS-SNP<sub>12</sub>/PET (68.1 Pa). Generally, a compromise needs to be achieved between these two important filtration-permeability parameters: high  $\eta$  and low  $\Delta p$ . To evaluate the overall filtration performance of the membranes, the quality factor (QF) is further calculated in figure 6(b), which also takes into account both the efficiency and the permeability. The results show that since the SiO<sub>2</sub> concentration is increased from 0 to 10 wt.%, the QF value is then improved from 0.0208 to 0.0281 Pa<sup>-1</sup>. However, when the concentration rises to 12 wt.%, the QF value begins to decrease slightly (0.0251 Pa<sup>-1</sup>). Besides, the two control samples (viscose/viscose/viscose and PET/PET/PET) exhibit relatively lower QF values, indicating the insufficient balance between breathability and filtration. Overall, the viscose/PS-SNP<sub>x</sub>/PET air filtration media has the best performance at 10 wt.% SiO<sub>2</sub> doping. It shows that this viscose/PS-SNP<sub>10</sub>/PET has good comprehensive filtration performance and great application prospects in the purification of PM2.5.

SiO<sub>2</sub> is considered a promising candidate for the design of new fibrous materials for air filtration because of excellent electret behavior, which can retain electric charges over a long period of time and create an external electric field [39, 40]. Furthermore, in the study of electrospinning fiber membranes, the introduction of SiO<sub>2</sub> provides the surface with a rougher structure, superhydrophobic property, and changes in fiber diameter and pore size [22, 23]. According to previous studies, inertial impaction, interception, and diffusion are the most important filtration mechanisms for air filtration according to classical filtration theory [41–43]. In this work,



the enhanced filtration performance could be attributed to the spatial-constructing ability of SiO<sub>2</sub> nanoparticles. During the filtration, a stagnant area will be formed in the boundary layer around the nano-protrusions modified rough fibers [31, 44, 45]. The fine particles move slowly like a peristaltic flow and stay at the edge of fibers. The rough structure improves the filtration efficiency and promotes air penetration through the membrane, which greatly improves the filtration performance. Additionally, the SiO<sub>2</sub> electret effect may be important to charge trapping and enhance the filtration properties [22, 29].

The filtration performance of commercial masks was also studied for the effective follow-up comparison with PS-SNP<sub>x</sub> fiber membranes. The experimental results are shown in table S2 and plotted in figure S3 (see supporting information). The QF of the viscose/PS-SNP<sub>10</sub>/PET air filtration media has a higher value than the commercial three-layered masks. Then the long-term filtration performance of air filtration was evaluated because it is significant for practical applications. As shown in figure S4 (see supporting information), after 8 h, the viscose/PS-SNP<sub>10</sub>/PET sample retains 92.1% of its initial filtration efficiency, showing long-term high stability, which is still higher than that of the tested commercial facial masks.

To the best of our knowledge, in addition to the air permeability property, the water-vapor permeability is also an important indicator of the parameters of membrane masks [46]. The water-vapor transmission rate (WVTR) could be measured and determined by the water-proof breathability [47]. As a result, the water-proof-breathable membrane is a kind of function material that can prevent the penetration of liquid water but allows water vapor/air to pass through, and it is widely used in protective clothing, chemical industries, and medical equipment [48]. It is reported that the electrospun fibrous membranes had good water-proof breathability [49, 50]. Besides, by introducing inorganic nano-SiO<sub>2</sub> to change the pore structure and hydrophobicity of the electrospun membranes, many studies have been carried out to enhance this performance [51–53]. The next step of this study will consist of performing the development and improvement of the water-vapor permeability of the novel PS-SNP fibrous membranes.

## 4. Conclusion

In summary, we developed novel and simple PS-SNP fibrous membranes utilizing electrospun PS fibers and SiO<sub>2</sub> nanoparticles for effective air filtration. The use of SiO<sub>2</sub> nanoparticles gives the fiber membrane superhydrophobicity and a relatively increased mechanical behavior compared with the pure PS membranes. More significantly, a composite PS-SNP fibrous membrane is assembled with the viscose and PET to be achieved a three-layered mask material. The as-prepared air filtration membrane has good air filtration, permeability performance and provides a general strategy for continuously exploring high-performance fiber media. It is concluded that the proposed PS-SNP air filtration membranes have high performance for filtering fine particulate matter. This fiber membrane-based mask provides new possibilities and concepts for existing masks on the market.

## Acknowledgments

The China Scholarship Council (CSC) is acknowledged for financial supports.

## Data availability statement

All data that support the findings of this study are included within the article (and any supplementary files).

## ORCID iDs

Dong Han  <https://orcid.org/0000-0002-9403-5209>

Jian Zhang  <https://orcid.org/0000-0002-6358-7158>

## References

- [1] Davdand P et al 2013 Maternal exposure to particulate air pollution and term birth weight: a multi-country evaluation of effect and heterogeneity *Environ. Health Perspect.* **121** 267–373
- [2] Xie Y, Zhao B, Zhang L and Luo R 2015 Spatiotemporal variations of PM 2.5 and PM 10 concentrations between 31 Chinese cities and their relationships with SO<sub>2</sub>, NO<sub>2</sub>, CO and O<sub>3</sub> *Particulology* **20** 141–9
- [3] Dominici F, Peng R D, Bell M L, Pham L, McDermott A, Zeger S L and Samet J M 2006 Fine particulate air pollution and hospital admission for cardiovascular and respiratory diseases *JAMA* **295** 1127–34
- [4] Wang G C and Wang P C 2014 PM 2.5 pollution in China and its harmfulness to human health *Science A Technology Review* **32** 72–8

- [5] Yin H, Pizzol M and Xu L 2017 External costs of PM 2.5 pollution in Beijing, China: uncertainty analysis of multiple health impacts and costs *Environ. Pollut.* **226** 356–69
- [6] Mehta P, McAuley D F, Brown M, Sanchez E, Tattersall R S, Manson J J and HLH Across Speciality Collaboration 2020 COVID-19: consider cytokine storm syndromes and immunosuppression *Lancet* **395** 1033
- [7] Bai Y, Yao L, Wei T, Tian F, Jin D Y, Chen L and Wang M 2020 Presumed asymptomatic carrier transmission of COVID-19 *JAMA* **323** 1406–7
- [8] Cao X 2020 COVID-19: immunopathology and its implications for therapy *Nat. Rev. Immunol.* **20** 269–70
- [9] Sun P, Lu X, Xu C, Sun W and Pan B 2020 Understanding of COVID-19 based on current evidence *Journal of Medical Virology* **92** 548–51
- [10] Wang X, Ding B, Yu J and Wang M 2011 Engineering biomimetic superhydrophobic surfaces of electrospun nanomaterials *Nano Today* **6** 510–30
- [11] Si Y, Yu J, Tang X, Ge J and Ding B 2014 Ultralight nanofibre-assembled cellular aerogels with superelasticity and multifunctionality *Nat. Commun.* **5** 1–9
- [12] Tan N P B, Paclijan S S, Ali H N M, Hallazgo C M J S, Lopez C J F and Eborá Y C 2019 Solution blow spinning (SBS) nanofibers for composite air filter masks *ACS Appl. Nano Mater.* **2** 2475–83
- [13] Liu C, Hsu P C, Lee H W, Ye M, Zheng G, Liu N and Cui Y 2015 Transparent air filter for high-efficiency PM 2.5 capture *Nat. Commun.* **6** 1–9
- [14] Wei X, Fei Y, Shi Y, Chen J, Lv B, Chen Y and Xiang H 2016 Hemocompatibility and ultrafiltration performance of PAN membranes surface-modified by hyperbranched polyesters *Polym. Adv. Technol.* **27** 1569–76
- [15] Wang N, Raza A, Si Y, Yu J, Sun G and Ding B 2013 Tortuously structured polyvinyl chloride/polyurethane fibrous membranes for high-efficiency fine particulate filtration *J. Colloid Interface Sci.* **398** 240–6
- [16] Zhu M, Hua D, Pan H, Wang F, Manshian B, Soenen S J and Huang C 2018 Green electrospun and crosslinked poly (vinyl alcohol)/poly (acrylic acid) composite membranes for antibacterial effective air filtration *J. Colloid Interface Sci.* **511** 411–23
- [17] Zhang L, Chen B, Ghaffar A and Zhu X 2018 Nanocomposite membrane with polyethyleneimine-grafted graphene oxide as a novel additive to enhance pollutant filtration performance *Environmental Science & Technology* **52** 5920–30
- [18] Liu F and Xu H 2017 Development of a novel polystyrene/metal-organic framework-199 electrospun nanofiber adsorbent for thin film microextraction of aldehydes in human urine *Talanta* **162** 261–7
- [19] Pattanauwat P, Tagaya M and Kobayashi T 2018 Controllable nanoporous fibril-like morphology by layer-by-layer self-assembled films of bioelectronics poly (pyrrole-co-formyl pyrrole)/polystyrene sulfonate for biocompatible electrode *Mater. Res. Bull.* **99** 260–7
- [20] Rajak A, Hapidin D A, Iskandar F, Munir M M and Khairurrijal K 2020 Electrospun nanofiber from various source of expanded polystyrene (EPS) waste and their characterization as potential air filter media *Waste Manage. (Oxford)* **103** 76–86
- [21] Buruga K, Kalathi J T, Kim K H, Ok Y S and Danil B 2018 Polystyrene-halloysite nano tube membranes for water purification *J. Ind. Eng. Chem.* **61** 169–80
- [22] Li X, Wang N, Fan G, Yu J, Gao J, Sun G and Ding B 2015 Electretted polyetherimide–silica fibrous membranes for enhanced filtration of fine particles *J. Colloid Interface Sci.* **439** 12–20
- [23] Zhong L, Wang T, Liu L, Du W and Wang S 2018 Ultra-fine SiO<sub>2</sub> nanofilament-based PMIA: a double network membrane for efficient filtration of PM particles *Sep. Purif. Technol.* **202** 357–64
- [24] Wan H, Wang N, Yang J, Si Y, Chen K, Ding B, Sun G, El-Newehy M, Al-Deyab S S and Yu J 2014 Hierarchically structured polysulfone/titania fibrous membranes with enhanced air filtration performance *J. Colloid Interface Sci.* **417** 18–26
- [25] Su J, Yang G, Cheng C, Huang C, Xu H and Ke Q 2017 Hierarchically structured TiO<sub>2</sub>/PAN nanofibrous membranes for high-efficiency air filtration and toluene degradation *J. Colloid Interface Sci.* **507** 386–96
- [26] Vanangamudi A, Hamzah S and Singh G 2015 Synthesis of hybrid hydrophobic composite air filtration membranes for antibacterial activity and chemical detoxification with high particulate filtration efficiency (PFE) *Chem. Eng. J.* **260** 801–8
- [27] Huang Z X, Liu X, Zhang X, Wong S C, Chase G G, Qu J P and Baji A 2017 Electrospun polyvinylidene fluoride containing nanoscale graphite platelets as electret membrane and its application in air filtration under extreme environment *Polymer* **131** 143–50
- [28] Guo Y, He W and Liu J 2020 Electrospinning polyethylene terephthalate/SiO<sub>2</sub> nanofiber composite needle felt for enhanced filtration performance *J. Appl. Polym. Sci.* **137** 48282
- [29] Ding X, Li Y, Si Y, Yin X, Yu J and Ding B 2019 Electrospun polyvinylidene fluoride/SiO<sub>2</sub> nanofibrous membranes with enhanced electret property for efficient air filtration *Composites Communications* **13** 57–62
- [30] Hosseini S A, Vossoughi M, Mahmoodi N M and Sadrzadeh M 2018 Efficient dye removal from aqueous solution by high-performance electrospun nanofibrous membranes through incorporation of SiO<sub>2</sub> nanoparticles *J. Clean. Prod.* **183** 1197–206
- [31] Wang N, Si Y, Wang N, Sun G, El-Newehy M, Al-Deyab S S and Ding B 2014 Multilevel structured polyacrylonitrile/silica nanofibrous membranes for high-performance air filtration *Sep. Purif. Technol.* **126** 44–51
- [32] Sun H, Xu Y, Zhou Y, Gao W, Zhao H and Wang W 2017 Preparation of superhydrophobic nanocomposite fiber membranes by electrospinning poly (vinylidene fluoride)/silane coupling agent modified SiO<sub>2</sub> nanoparticles *J. Appl. Polym. Sci.* **134** 13
- [33] Zhang Q, Yang H and Fu Q 2004 Kinetics-controlled compatibilization of immiscible polypropylene/polystyrene blends using nano-SiO<sub>2</sub> particles *Polymer* **45** 1913–22
- [34] Gao X, Zhao T, Luo G, Zheng B, Huang H, Ma R, Han X and Chai Y 2018 Enhanced thermal and mechanical properties of PW-based HTPB binder using polystyrene (PS) and PS-SiO<sub>2</sub> microencapsulated paraffin wax (MePW) *J. Appl. Polym. Sci.* **135** 46222
- [35] Okada A and Usuki A 2006 Twenty years of polymer-clay nanocomposites *Macromol. Mater. Eng.* **291** 1449–76
- [36] Mao X, Si Y, Chen Y, Yang L, Zhao F, Ding B and Yu J 2012 Silica nanofibrous membranes with robust flexibility and thermal stability for high-efficiency fine particulate filtration *RSC Adv.* **2** 12216–23
- [37] Yan J, Han Y, Xia S, Wang X, Zhang Y, Yu J and Ding B 2019 Polymer template synthesis of flexible BaTiO<sub>3</sub> crystal nanofibers *Adv. Funct. Mater.* **29** 1907919
- [38] Verdager A, Weis C, Oncins G, Ketteler G, Bluhm H and Salmeron M 2007 Growth and structure of water on SiO<sub>2</sub> films on Si investigated by kelvin probe microscopy and *in situ* x-ray spectroscopies *Langmuir* **23** 9699–703
- [39] Mescheder U, Müller B, Baborie S and Urbanovic P 2009 Properties of SiO<sub>2</sub> electret films charged by ion implantation for MEMS-based energy harvesting systems *J. Micromech. Microeng.* **19** 094003
- [40] Günther P and Xia Z 1993 Transport of detrapped charges in thermally wet grown SiO<sub>2</sub> electrets *J. Appl. Phys.* **74** 7269–74
- [41] Gong G, Zhou C, Wu J, Jin X and Jiang L 2015 Nanofibrous adhesion: the twin of gecko adhesion *ACS Nano* **9** 3721–7
- [42] Viswanathan G, Kane D B and Lipowicz P J 2004 High efficiency fine particulate filtration using carbon nanotube coatings *Adv. Mater.* **16** 2045–9

- [43] Li P, Wang C, Zhang Y and Wei F 2014 Air filtration in the free molecular flow regime: a review of high-efficiency particulate air filters based on carbon nanotubes *Small* **10** 4543–61
- [44] Hosseini S A and Tafreshi H V 2011 On the importance of fibers' cross-sectional shape for air filters operating in the slip flow regime *Powder Technol.* **212** 425–31
- [45] Hosseini S A and Tafreshi H V 2010 Modeling particle filtration in disordered 2D domains: a comparison with cell models *Sep. Purif. Technol.* **74** 160–9
- [46] Chen L, Wu F, Li Y, Wang Y, Si L, Lee K I and Fei B 2018 Robust and elastic superhydrophobic breathable fibrous membrane with *in situ* grown hierarchical structures *J. Membr. Sci.* **547** 93–8
- [47] Kang Y K, Park C H, Kim J and Kang T J 2007 Application of electrospun polyurethane web to breathable water-proof fabrics *Fibers Polym.* **8** 564–70
- [48] Mukhopadhyay A and Midha V K 2008 A review on designing the waterproof breathable fabrics: I. Fundamental principles and designing aspects of breathable fabrics *J. Ind. Text.* **37** 225–62
- [49] Zhao J, Li Y, Sheng J, Wang X, Liu L, Yu J and Ding B 2017 Environmentally friendly and breathable fluorinated polyurethane fibrous membranes exhibiting robust waterproof performance *ACS Appl. Mater. Interfaces* **9** 29302–10
- [50] Ju J, Shi Z, Deng N, Liang Y, Kang W and Cheng B 2017 Designing waterproof breathable material with moisture unidirectional transport characteristics based on a TPU/TBAC tree-like and TPU nanofiber double-layer membrane fabricated by electrospinning *RSC Adv.* **7** 32155–63
- [51] Sheng J, Xu Y, Yu J and Ding B 2017 Robust fluorine-free superhydrophobic amino-silicone oil/SiO<sub>2</sub> modification of electrospun polyacrylonitrile membranes for waterproof-breathable application *ACS Appl. Mater. Interfaces* **9** 15139–47
- [52] Su C, Chang J, Tang K, Gao F, Li Y and Cao H 2017 Novel three-dimensional superhydrophobic and strength-enhanced electrospun membranes for long-term membrane distillation *Sep. Purif. Technol.* **178** 279–87
- [53] Liang Y, Ju J, Deng N, Zhou X, Yan J, Kang W and Cheng B 2018 Super-hydrophobic self-cleaning bead-like SiO<sub>2</sub>@PTFE nanofiber membranes for waterproof-breathable applications *Appl. Surf. Sci.* **442** 54–64